Mühendislik Bilimleri ve Tasarım Dergisi
10(4), 1194 – 1211, 2022
e-ISSN: 1308-6693

Journal of Engineering Sciences and Design
DOI: 10.21923/jesd.1106646

Araştırma Makalesi Research Article

# THE EFFECT OF USING PHASE CHANGE MATERIALS AND EXAMINING THE ASPECT RATIO IN AN AIR-COOLED SYSTEM OF A PLATE BATTERY CONNECTED TO A SOLAR SYSTEM

**Nevzat AKKURT**[*]

Munzur Üniversitesi, Mühendislik Fakültesi, Makine Mühendisliği Bölümü, 62000 Tunceli, Türkiye

**Keywords**

*PCM,*
*Plate-Type Battery,*
*Building,*
*Energy Consumption,*
*Air-Cooled.*

**Abstract**

Lithium-ion batteries are widely used in the electronics industry to store electrical energy. One of the challenges with these batteries is that they heat up during operation, which can damage the battery. For this reason, this paper simulates the cooling process of a plate-type (BTP) lithium-ion battery pack. To control the temperature of the battery (T-B), a laminar air flow and a phase change material (PCM) are used. The PCM is placed in a heat sink around the battery. This evaluation is performed temporarily for four different dimensions of the PCM pack. The hot outlet of this system is used to provide the thermal energy required for a small residential building (THE) at a mild temperature. The BTP was also simulated using COMSOL. The results show that the use of larger heat sinks can increase the maximum (MAX) and average (AVE) temperature of the battery. The minimum T-B occurs at different times for the smaller PCM heat sinks. Also, when using a heatsink with a larger PCM volume, it takes longer for the PCM to fully solidify. A BTP with 5 or 50 battery cells can provide up to 3% or 30% of the THE required for the building.

# GÜNEŞ SİSTEMİNE BAĞLI PLAKA PİL HAVA SOĞUTMALI BİR SİSTEMDE FAZ DEĞİŞİM MALZEMELERİ KULLANILMASI VE GÖRÜNÜŞ ORANININ İNCELENMESİ ETKİSİ

**Anahtar Kelimeler**

*Faz Değiştiren malzemeler*
*Plaka Tipi Pil,*
*Bina,*
*Enerji tüketimi,*
*Hava soğutmalı.*

**Öz**

Lityum iyon piller, elektronik endüstrisinde elektrik enerjisini depolamak için yaygın olarak kullanılmaktadır. Bu pillerin zorluklarından biri, çalışma sırasında pile zarar verebilecek şekilde ısınmalarıdır. Bu sorundan dolayı, bu çalışmada plaka tipi lityum iyon pil takımının (BTP) soğutma süreci simüle edilmiştir. Pilin (T-B) sıcaklığını kontrol etmek için laminer hava akımı ve faz değiştirme malzemesi (PCM) kullanılır. PCM, pilin etrafındaki bir soğutucunun içine yerleştirilmiştir. Mevcut değerlendirme, PCM paketinin dört farklı boyutu için geçici olarak yapılır. Bu sistemin çıkış sıcaklığı, ılıman bir sıcaklıkta küçük bir konut binası için gerekli olan termal enerjiyi (THE) sağlamak için kullanılır. BTP ayrıca COMSOL kullanılarak simüle edilmiştir. Sonuçlar, daha büyük soğutucu pillerin kullanımının pilin maksimum (MAX) ve ortalama (AVE) sıcaklıklarını artırabileceğini gösterdi. Minimum T-B, daha küçük PCM soğutucusunda farklı zamanlarda meydana gelir. Ayrıca, daha büyük PCM hacmine sahip bir soğutucu kullanmak, PCM'nin tamamen katılaşması için daha uzun sürer. 5 ve 50 pil hücreli bir BTP, binanın ihtiyaç duyduğu THE'nin sırasıyla %3'ünü ve %30'unu sağlayabilir.

Akkurt, N., (2022). The Effect Of Using Phase Change Materials And Examining The Aspect Ratio In An Air-Cooled System Of A Plate Battery Connected To A Solar System, Journal of Engineering Sciences and Design, 10(4), 1194-1211.

[*] İlgili yazar / Corresponding author: nakkurt@munzur.edu.tr, +90-428-213-17-94

Yazar Kimliği / Author ID (ORCID Number)
N. Akkurt, 0000-0001-5550-1265

Makale Süreci / Article Process

| | |
|---|---|
| Başvuru Tarihi / Submission Date | 20.04.2022 |
| Revizyon Tarihi / Revision Date | 29.06.2022 |
| Kabul Tarihi / Accepted Date | 29.06.2022 |
| Yayım Tarihi / Published Date | 30.12.2022 |


## 1. Introduction

Compared to other types of batteries, lithium-ion batteries are used in various industries, including electric vehicles, due to their suitable thermal capacity, relatively long lifetime, and low discharge rate. However, there are several challenges in using these batteries, such as their thermal stability or explosion due to overheating or uneven heat distribution (Al-Zareer et al., 2017; Amalesh and Lakshmi Narasimhan, 2020; Bibin et al., 2020; Elsheikh et al., 2014). Therefore, the design and application of battery cooling system and thermal management are important to provide suitable and safe working conditions. In recent years, the idea of introducing electric and hybrid electric vehicles and fuel cells has attracted much interest in the industry to replace internal combustion engine vehicles. This generation of vehicles has a battery to store energy. Electric vehicles are similar in many ways to gasoline and diesel vehicles. The only difference is the replacement of the internal combustion engine with a rechargeable battery (Hannan et al., 2014; Lopes et al., 2010; Nilsson, 2011; Sanguesa et al., 2021; Sun et al., 2019).

The electric motor is powered by the battery, and the battery drives the wheels. Batteries are generally the most widely used form of energy storage technology due to their low cost, mobility, and ability to function in a variety of situations. Batteries generate electricity by releasing energy that has been stored in chemicals. Because of their lower cost, longer life, and better energy density, lithium-ion batteries are becoming increasingly popular in electric cars. Significant breakthroughs in lithium-ion battery technology have enabled industry owners and technological pioneers to bring new products to market, including satellites and spacecraft, space stations, electric and hybrid cars, and advanced communications equipment. In addition, the technology used in the metallurgy of this type of batteries has led to the introduction of flexible and curved batteries into the market (Jiang et al., 2022; Orooji et al., 2022; Tran et al., 2022; Xie et al., 2021; Zhang, J. et al., 2022; Zhang, Y.S. et al., 2022). It should be noted that the thermal problems of these batteries have limited their applicability for high energy consumption, as high operating temperatures in these batteries can significantly reduce their lifetime and even cause burns and fires. In general, the best performance of lithium-ion batteries is determined solely by their temperature, as these batteries are very sensitive to operating temperature and must be operated within a certain temperature range (An et al., 2017; Karimi and Li, 2013; Khateeb et al., 2005; Pesaran, 2001; Qian et al., 2016; Yang et al., 2019). These batteries have a MAX working temperature of 45 °C. It has been emphasized that they should not exceed a safe temperature of 60 degrees Celsius. Therefore, many researchers are interested in studying the thermal management systems of these batteries, and numerous studies have been conducted on practical high-efficiency cooling systems for thermal management of these devices (Hajatzadeh Pordanjani et al., 2019; Pordanjani et al., 2021; Pordanjani et al., 2019). Various methods such as air cooling, liquid cooling, nanofluids, heat pipes, and the use of PCMs have been proposed to provide the desired thermal management conditions and maintain the temperature of the batteries within a normal and safe range (Huang et al., 2021; Kirad and Chaudhari, 2021; Shen et al., 2021; Yao et al., 2021; Zhang, X. et al., 2022; Zichen and Changqing, 2021). A review of researches on encapsulation of organic phase change materials, thermal conductivity enhancement and modeling of thermal behavior reported in the last 20 years has presented by (Mert et al., 2018 ). (Gürbüz et al., 2021) conducted a numerical analysis of the melting and solidification processes of the thermal energy storage (TES) system designed for the exhaust waste heat recovery of a spark-ignition engine was performed. Paraffin wax, which stores thermal energy as latent heat and is commercially identified with the code RT35, is used as phase change material in the thermal energy storage (TES) system. Sisk et al. (Sisk et al., 2015) summarized the electrochemical and thermal models of the battery. COMSOL software was used for the electrochemical modeling. The dynamic resistance of the battery was one of the most important properties studied in this simulation. Based on the results and comparison with the static resistance of the battery, it was found that the thermal load was overestimated in the design phase. Shojaei et al. (Shojaei et al., 2016) evaluated the battery as a component of the vehicle from a systematic point of view to cool the battery of the hybrid vehicle. They evaluated passenger compartment cooling, internal combustion engine cooling, and battery cooling. Due to the complexity of the model, numerous assumptions were made, such as neglecting spatial effects in the battery or the cabin.

Thermal resistance, heat generation, radiation, and convective heat transfer were considered in the numerical models. Singh et al. (Singh et al., 2021) studied forced airflow in the BTP and found that using different designs did not affect the MAX -T-B. Shi et al. (Shi et al., 2021) studied the cooling system by optimizing the airflow in the BTP using an artificial neural network. They demonstrated a device with three outputs that can reduce the temperature of the BTP by up to 6 degrees Celsius.

Khateeb et al. (Khateeb et al., 2004) evaluated the thermal management system of a lithium-ion battery cooled with PCMs. They used air to charge and discharge the PCMs. The BTP consisted of nine 18650 batteries. They designed the battery for different conditions and showed that PCMs are a good alternative to cooling systems. In one of the studies conducted using the active method, Wang et al. (Wang et al., 2014) investigated the optimal arrangement of cells in the BTP. They also evaluated the effects of the location of the air inlet and outlet. They investigated the thermal behavior of the battery module at different flow rates, different charging rates, and different operating temperatures. Using air for cooling was not suitable in many cases due to the weak thermal properties of air and caused the T-B to exceed its allowable temperature. Therefore, some researchers used liquids to cool the battery to improve the cooling rate.

Huo et al. (Huo and Rao, 2015) numerically evaluated the effect of adding alumina nanoparticles to the base fluid. The addition of nanoparticles can lower the MAX temperature of battery cells. Their results showed that the MAX cell temperature could be reduced by 7% by using a nanofluid with a volume fraction of 4%. Using waste energy to provide the energy needed for heating can reduce energy consumption and decrease fossil fuel consumption. One of the devices that generate unwanted heat is batteries. Batteries come in a variety of shapes and sizes, including those that can be alternately charged and discharged. These batteries are used in various devices, such as electric cars and solar vehicles, electronic devices, etc. On the other hand, a considerable amount of energy is consumed annually to heat a residential house in the world. Therefore, reducing energy consumption in buildings can be very important. In this paper, the effect of using the heat generated by a BTP to heat a building is studied. The BTP consists of plate batteries and a PCM pack placed around the batteries in a rectangular enclosure. The batteries are placed in the air duct, and the effects of different dimensions of the PCM pack on the T-B and delivered energy of the house are estimated at different times.

## 2. Problem definition

As shown in Fig. 1, a BTP with plate-type lithium-ion battery cells is housed in an air vent. Each battery cell is in a separate channel. To reduce the computation time, only one battery cell is simulated. A no-slip boundary condition applies to the walls of these ducts. Air enters the ducts at constant temperature and velocity with a Reynolds number (Re) of 150 and exits at atmospheric pressure. A rectangular PCM heat sink is placed around all battery cells. Four models of the heat sink with different thicknesses are considered. (Kant et al. 2017) is used for the PCM properties used in this study.

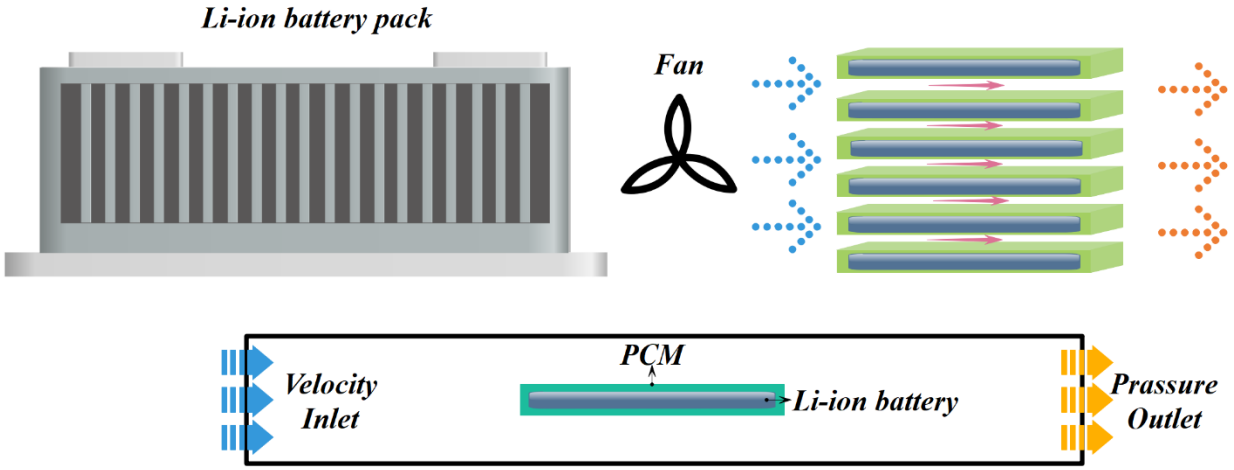


**Figure. 1**. A schematic of the battery cooling system and different types of heatsink used for PCM.

The battery cooling system is used in the air conditioning system of a 48 m2 building. The house consists of two rooms and a kitchen. It is located in a mild climate in the northern hemisphere. The materials used were selected based on the study (Alqaed, 2022). Figure. 2 shows a schematic diagram of the building and its climate system.

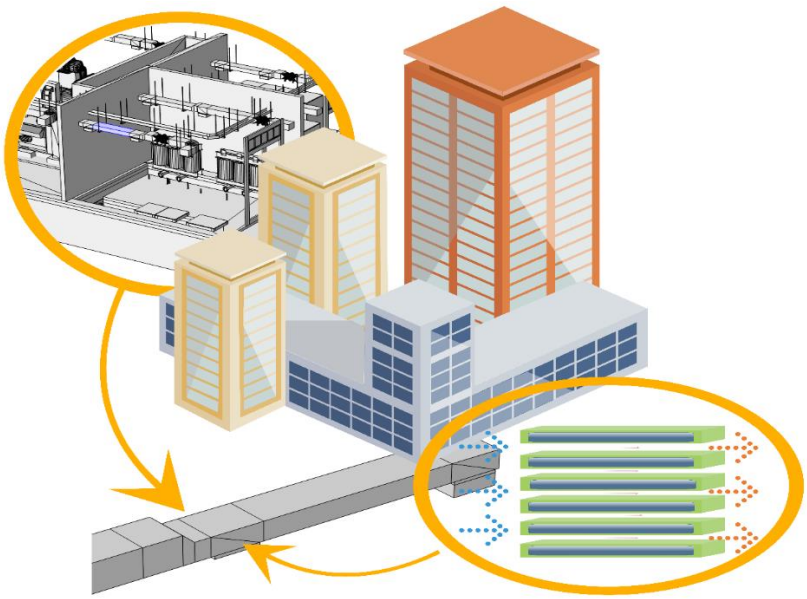

**Figure. 2**. The building studied and its ventilation system.

### 2.1. Governing equations

The air enters the duct with constant temperature and velocity and exits the other side with constant pressure. After solving the battery equations, which appear as source terms in the energy equation, heat is generated inside the battery, causing the PCM to melt. The PCM leads to a uniform temperature distribution on the battery surface.

$$\rho c_p \frac{\partial T}{\partial t} = \frac{\lambda_r}{r}\frac{\partial}{\partial r}\left(r\frac{\partial T}{\partial r}\right) + \frac{\lambda_\varphi}{r^2}\frac{\partial^2 T}{\partial \varphi^2} + \lambda_Z \frac{\partial^2 T}{\partial z^2} + Q \tag{1}$$

Where Q is the current generated in the battery and λ is the thermal conductivity. Also, ρ and c_p are the density and heat capacity, respectively. (Bernardi et al., 1985) showed that the amount of heat flow in the battery can be calculated as follows:

$$Q = I[(U_{OCV} - U) + IT\frac{\partial U_{OCV}}{\partial T}] \tag{2}$$

This equation includes two types of heat generated in the battery: heat generated by Joule resistance and heat generated by entropy and electrochemical reaction in the battery. I is the charge and discharge current and U_OCV is the open circuit voltage. Therefore, the equation for heat generation in the battery is written as follows:

$$q = \frac{I}{V}[(U_{OCV} - U) + T\frac{\partial U_{OCV}}{\partial T}] = \frac{I}{V}\left(IR_j + T\frac{\partial U_{Ocv}}{\partial T}\right) \tag{3}$$

The enthalpy-porosity method is used for numerical modelling of the solid-liquid phase change. In this method, the computational domain is a porous region such that the value of the porosity coefficient is equal to one in the liquid phase and zero in the solid phase. The solid-liquid interface forms a mushy region where the porosity coefficient varies between zero and one. In this method, a fixed grid is used and the location of the solid-liquid interface is determined implicitly at each time point (Kalbasi, 2021; Kalbasi et al., 2019). The following continuity, momentum, and energy equations are established:

$$\frac{\partial u}{\partial x} + \frac{\partial v}{\partial y} = 0 \tag{4}$$

$$\rho\left(\frac{\partial u}{\partial t} + u\frac{\partial u}{\partial x} + v\frac{\partial u}{\partial y}\right) = -\frac{\partial p}{\partial x} + \mu\left(\frac{\partial^2 u}{\partial x} + \frac{\partial^2 u}{\partial y}\right) + \rho g\beta\, cos(\theta)\,(T - T_m) + Au \tag{5}$$

$$\rho\left(\frac{\partial v}{\partial t} + u\frac{\partial v}{\partial x} + v\frac{\partial v}{\partial y}\right) = -\frac{\partial p}{\partial y} + \mu\left(\frac{\partial^2 v}{\partial x} + \frac{\partial^2 v}{\partial y}\right) + \rho g\beta\, sin(\theta)\,(T - T_m) + Av \tag{6}$$

Here, $A$ is the porosity function:

$$A = -C\frac{(1-\gamma)^2}{\gamma^3+\varepsilon} \tag{8}$$

where c = $10^6$ is a mushy constant. Also, $\varepsilon$ is $10^{-3}$ to avoid dividing the above fraction by zero when the amount of liquid fraction is zero. The liquid fraction is also calculated using the following equation:

$$\gamma = \frac{\Delta H}{L_{sf}} = \begin{cases} 0 & if \quad T < T_{solidus} \\ \dfrac{T - T_{solidus}}{T_{Liquidus} - T_{solidus}} & if \quad T_{Liquidus} < T < T_{solidus} \\ 1 & if \quad T > T_{Liquidus} \end{cases} \tag{9}$$

Energy conservation equation:

$$\rho\left(\frac{\partial}{\partial t}(c_P T) + \frac{\partial}{\partial x}(c_P u T) + \frac{\partial}{\partial y}(c_P v T)\right) = \frac{\partial}{\partial x}\left(k\frac{\partial T}{\partial x}\right) + \frac{\partial}{\partial y}\left(k\frac{\partial T}{\partial y}\right) - S_T \tag{10}$$

$$S_T = \rho\left(\frac{\partial}{\partial t}(\Delta H) + \frac{\partial}{\partial x}(u\Delta H) + \frac{\partial}{\partial y}(v\Delta H)\right) \tag{11}$$

Two-dimensional continuity and momentum equations for a Newtonian fluid are introduced. A laminar, incompressible and steady flow is assumed. Body forces such as gravity. The continuity equations and the x and y components of the momentum equations are as follows:

$$\frac{\partial u}{\partial x} + \frac{\partial v}{\partial y} = 0 \tag{12}$$

$$\rho\left(u\frac{\partial u}{\partial x} + v\frac{\partial u}{\partial y}\right) = -\frac{\partial p}{\partial x} + \mu\left(\frac{\partial^2 u}{\partial x^2} + \frac{\partial^2 u}{\partial y^2}\right) \tag{13}$$

$$\rho\left(u\frac{\partial v}{\partial x} + v\frac{\partial v}{\partial y}\right) = -\frac{\partial p}{\partial y} + \mu\left(\frac{\partial^2 v}{\partial x^2} + \frac{\partial^2 v}{\partial y^2}\right) \tag{14}$$

## 3. Numerical method

To solve the equations, discrete equations must be established. Therefore, the equations for air flow, phase change PCM, and battery equations are discretized. There are several methods to discretize equations, and researchers are still searching for new methods. In this paper, the finite element method is used to discretize the equations. COMSOL Multiphysics software, version 5.6, is used to solve the discrete equations. To calculate the heat load of the building and evaluate the impact of the heat of the batteries on the energy supply of the house, the Design Builder software is used.

After discretizing the equations, it is necessary to solve the discrete equations at points on the geometry. Therefore, a grid is created on the geometry. Due to the importance of solving the PCM phase change and the battery, a fine grid is used for these two parts and a normal grid for the channel. Finally, the number of elements used is 965,382 elements. Table 1 shows the AVE -T-B and the volume fraction of the melt PCM for different number of elements. From the table, it can be seen that the selected number of elements is acceptable in terms of computational time.

**Table 1**. AVE-T-B and volume fraction of molten PCM for a different number of elements and computational time for the largest PCM heatsink.

| No. of elements | 610834 | 793864 | 965382 | 1258640 |
|---|---|---|---|---|
| Computational time | 16 min | 50 min | 110 min | 260 min |
| AVE battery temperature | 303.67 | 303.98 | 304.07 | 304.09 |
| Volume fraction of molten PCM | 47.67 | 47.44 | 47.31 | 47.30 |

## 4. Validation

A similar article is selected to confirm the present results. (Almehmadi et al., 2022) studied the effects of using a battery heater to heat a building. A cylindrical battery was used. The T-B quantities determined in the present work are compared with those of (Almehmadi et al., 2022) at different velocities and times (Fig. 3). From the table,

it can be seen that the error MAX between the present work and the study of (Almehmadi et al., 2022) is less than 4%, which is indicative of the accuracy of the present simulations.

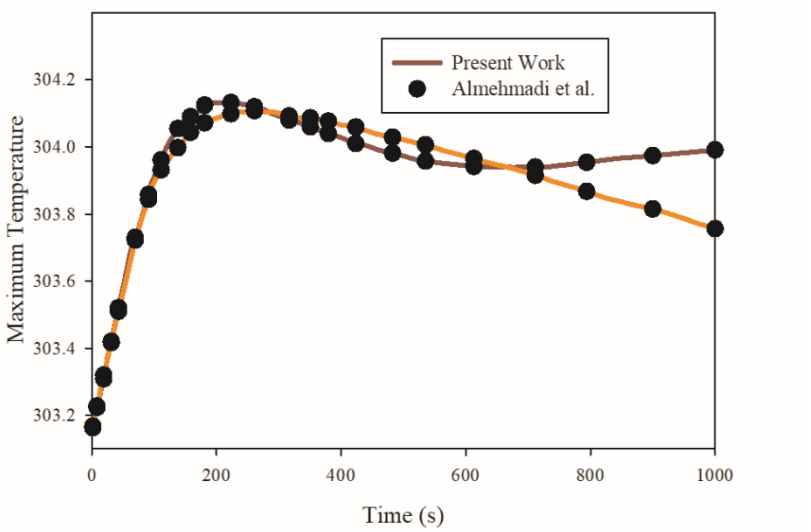


**Figure. 3**. Comparison of T-B obtained from the present work with those reported by (Almehmadi et al., 2022) at different velocities.

## 4. Results and discussion

The velocity contours are shown in Fig. 4 for different models of the heat sink PCM. The change of velocity during the collision with the heat sink and the battery depends on the dimensions of the heat sink. When more PCM is used in the heat sink, the amount of velocity changes is higher, but when the heat sink is smaller (model 1), the amount of velocity changes is lower. A larger heat sink also results in the velocity of MAX being slightly higher than with a smaller heat sink.

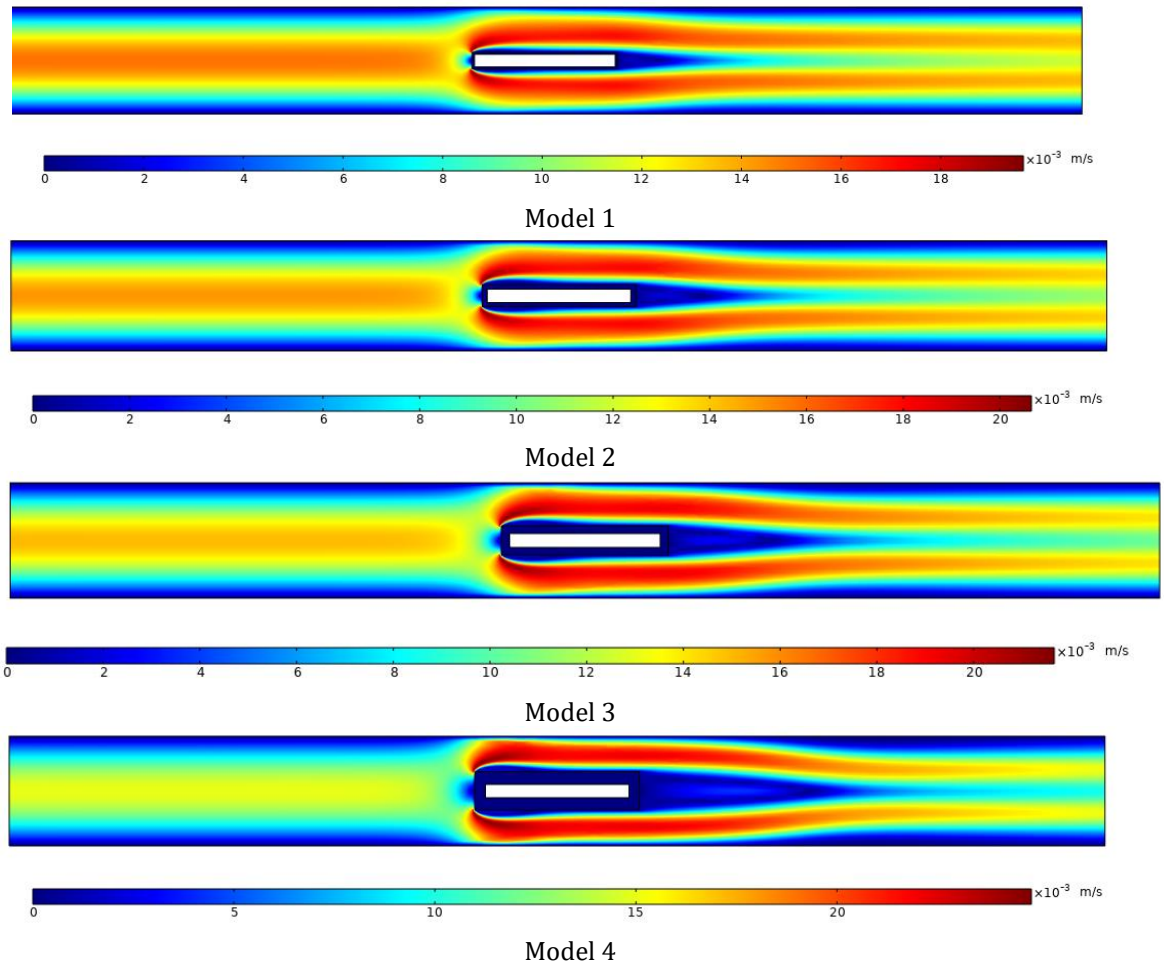


**Figure. 4**. velocity contour for different cavity models filled with phase change materials with different aspect ratios.

Figure. 5 illustrates the phase change of PCM at different times for different models of the PCM heat sink. The amount of PCM used in the heat sink affects its solidification time. The more PCM used in the heat sink, the longer it takes for PCM to solidify completely. Therefore, in Model 4, a significant amount of molten PCM remains over time, while in Model 1, all PCM solidifies in a short time. The solidification of PCM starts at the point where the air collides with the side of the battery. Then the parts of the heat sink that are exposed to more air become solid. Due to the heat generation in the battery, the PCM on the side of the battery becomes solid later than the other parts.

250sec

500sec

750sec

1000sec
Model 1

250sec

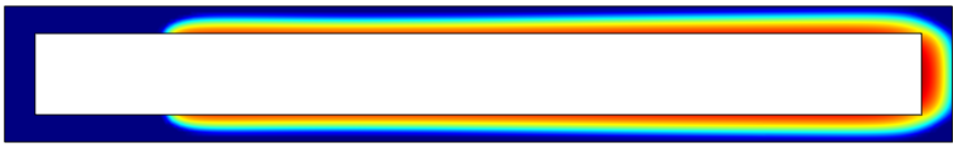

500sec

750sec

1000sec
Model 2

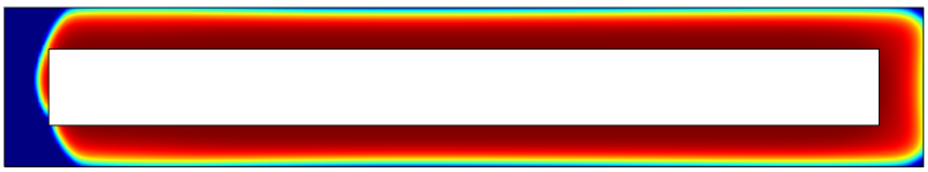

250sec

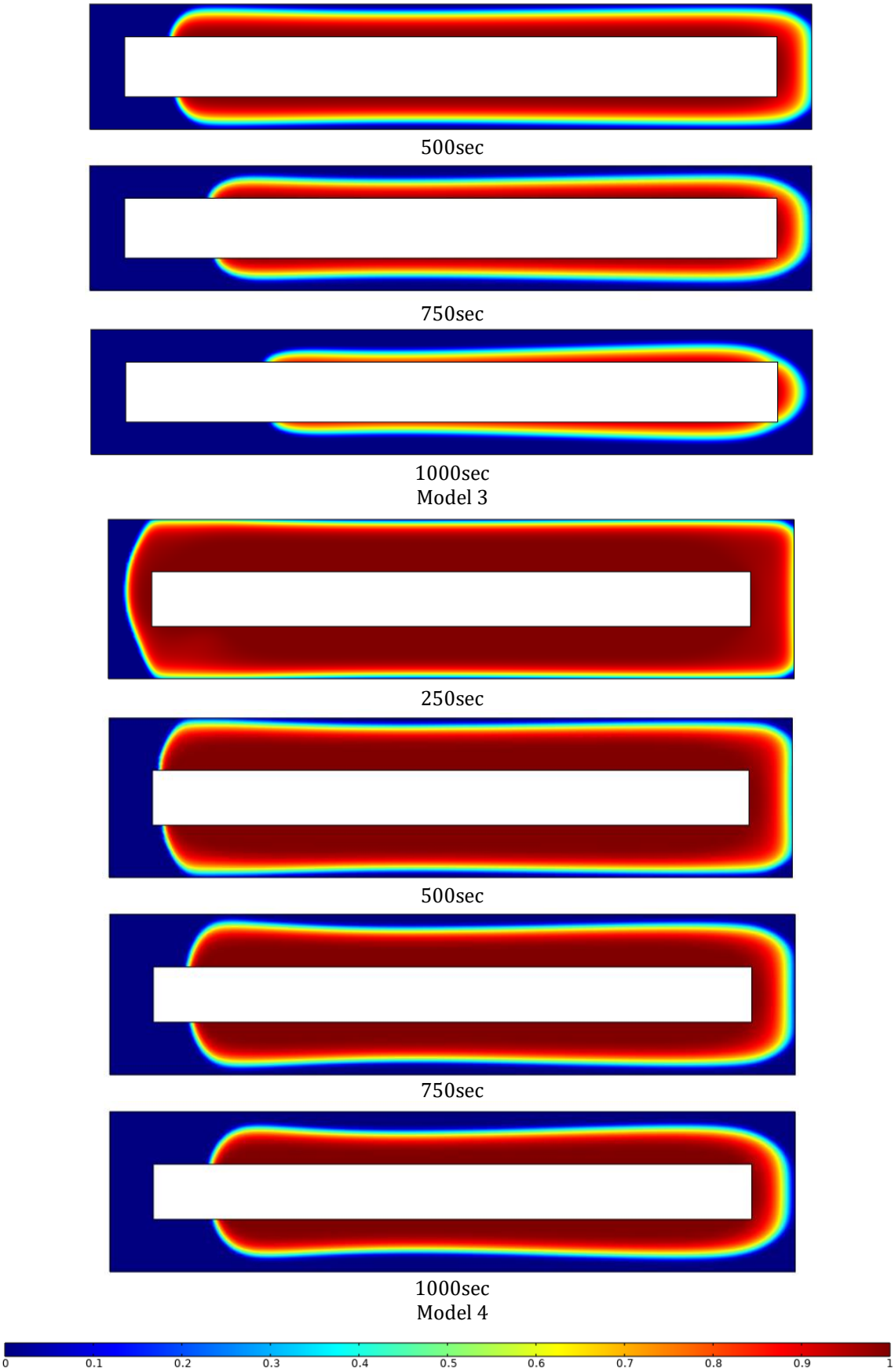


**Figure. 5**. The amount of PCM for different cavity models filled with phase change materials with different aspect ratios.

Figure. 6 illustrates the temperature profiles at different times for different models of the PCM heat sink. The cold air meets the battery at the inlet and its temperature is increased by the cooling of the battery. Due to the horizontal

position of the battery in the air duct, the T-B at the inlet is reduced. The battery has a lower temperature at the inlet and a higher temperature at the outlet. The PCM heat sink solidifies first at the inlet and then at the outlet. For heat sink models with a higher percentage of PCM, e.g., Model 4, the temperature changes slightly over time, and the melt PCM does not allow T-B and PCM to be reduced. However, in Model 1, where less PCM is used in the heat sink, T-B and heat sink increase over time. The larger the amount of heat sink, the smaller the temperature changes over time.

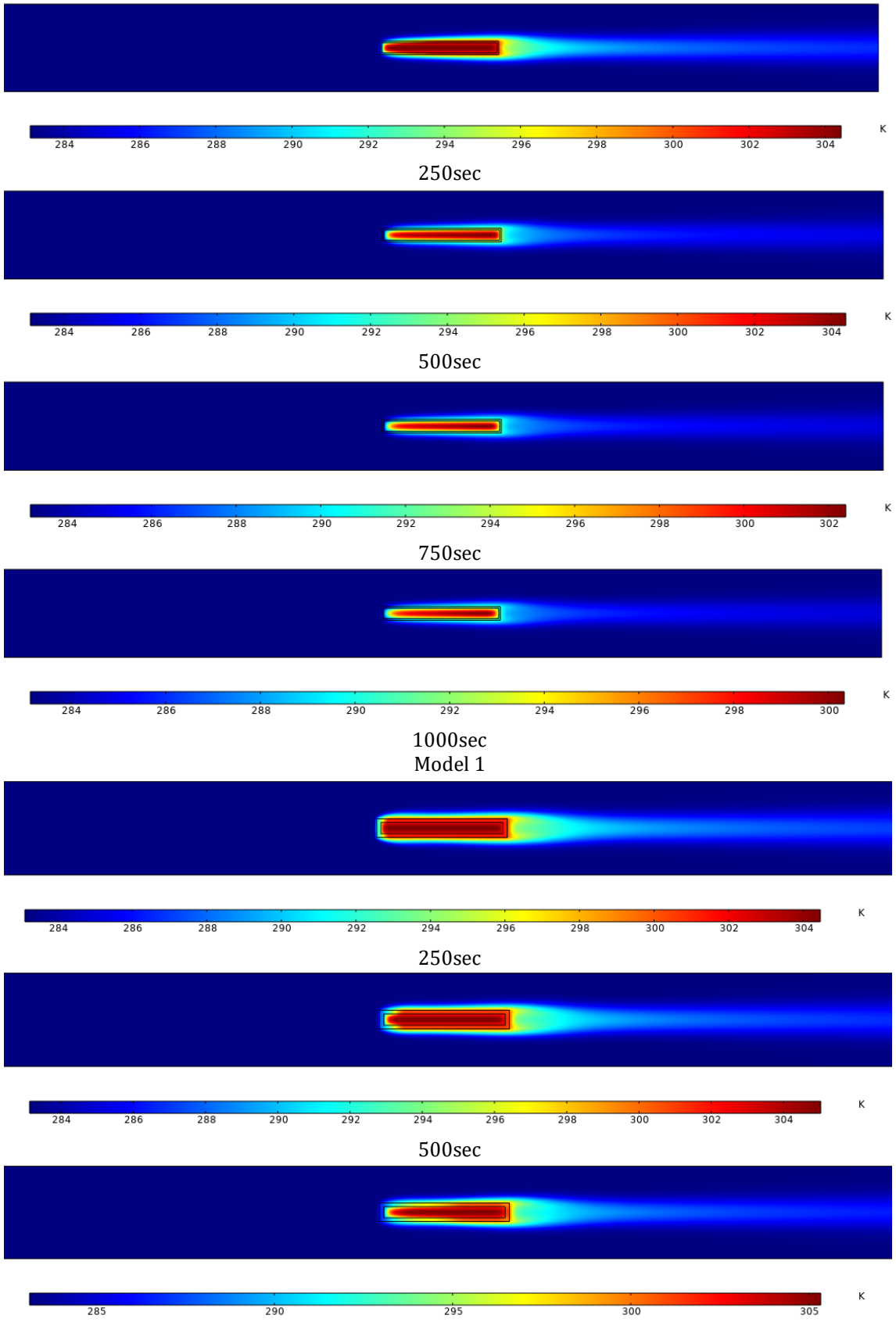

750sec

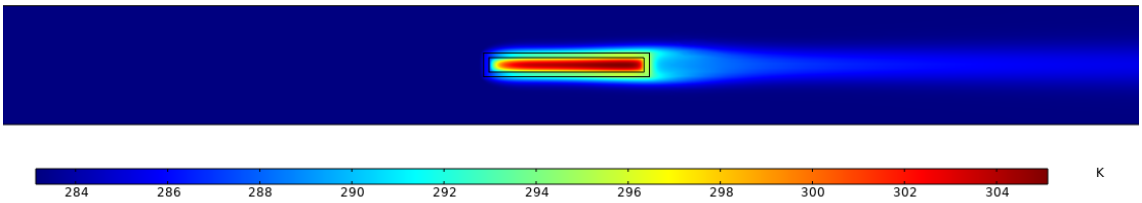


1000sec
Model 2

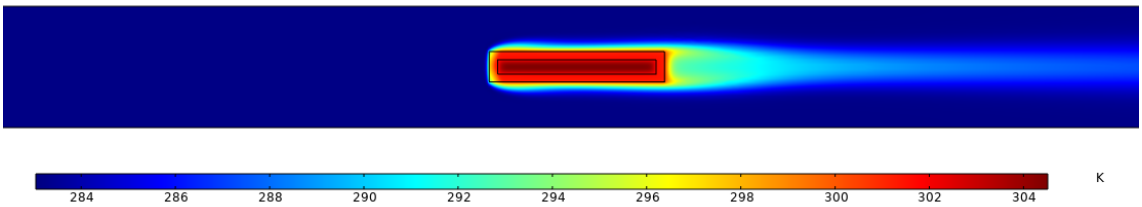


250sec

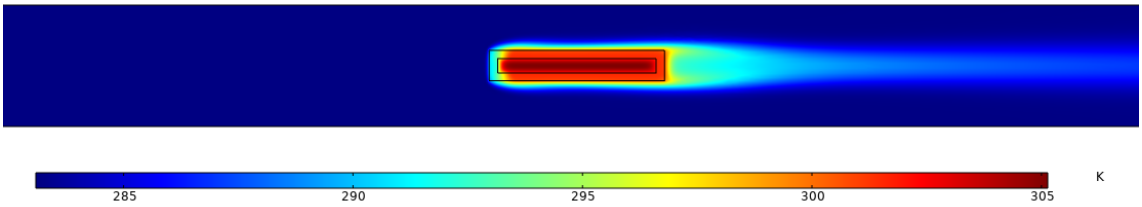


500sec

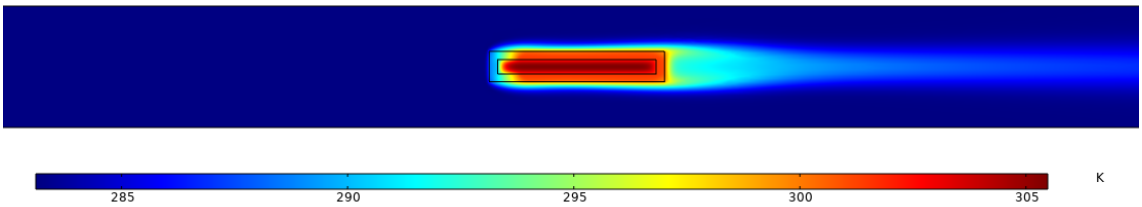


750sec

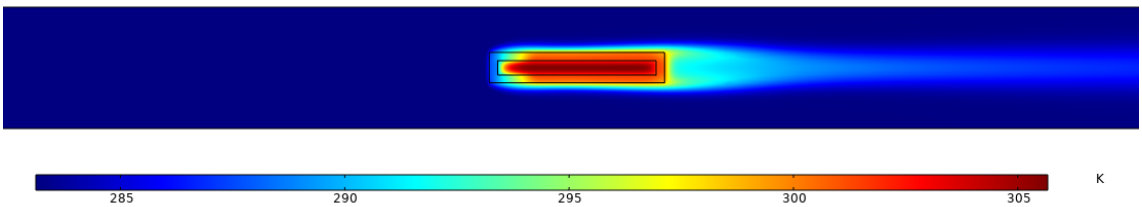


1000sec
Model 3

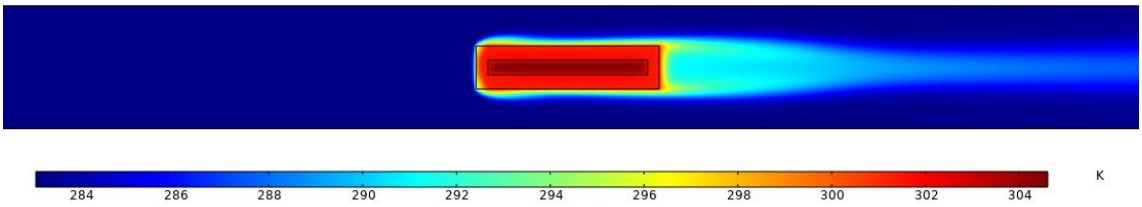


250sec

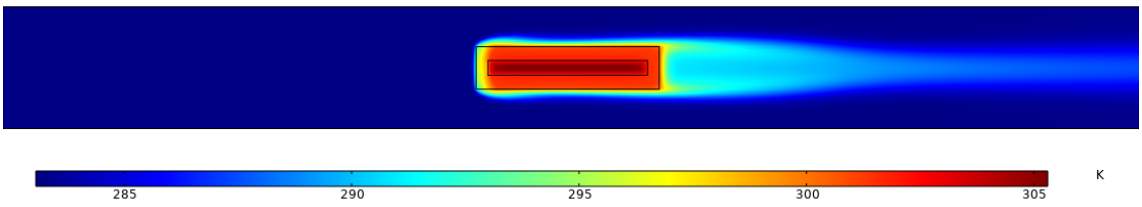


500sec

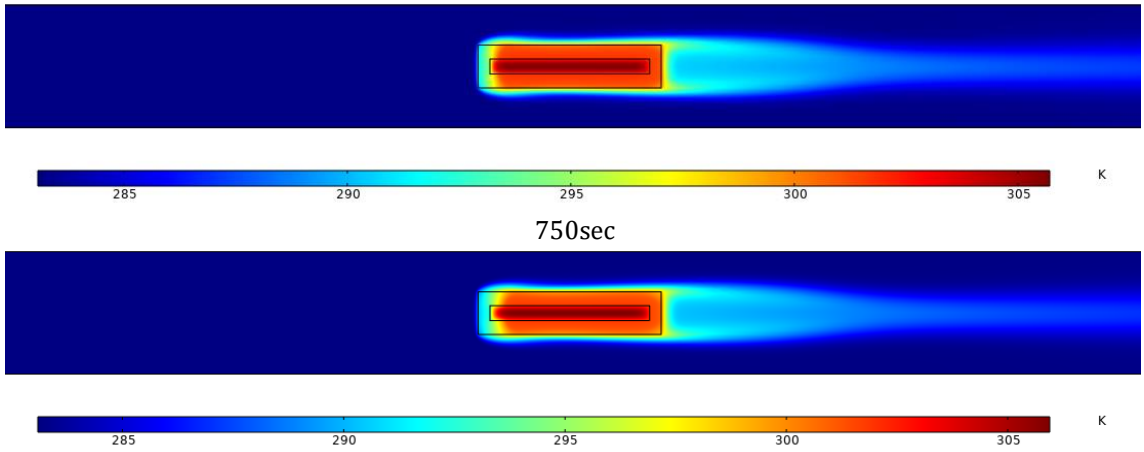


**Figure.6**. The temperature contours for different cavity models filled with phase change materials with different aspect ratios.

Figure. 7 shows the AVE T-B at different times for different PCM heat sink models. T-B is increased by the chemical reactions in the battery. The chemical reactions show up as heat flow. This heat should be dissipated from the battery, otherwise it will cause an excessive increase due to the heat buildup in the battery. As a result, the battery will burn or explode in a short time. Due to the presence of molten PCM around the battery, the heat transfer rate from the battery to the air is low. This is the most critical condition for passive temperature management. When the PCM is completely melted and can no longer manage the T-B, the air solidifies the PCM, dissipating the excess heat so that it can effectively manage the T-B . The higher the PCM in the heat sink (Model 4), the higher the T-B. For Model 1, where the amount of PCM is lower, the T-B is smaller.

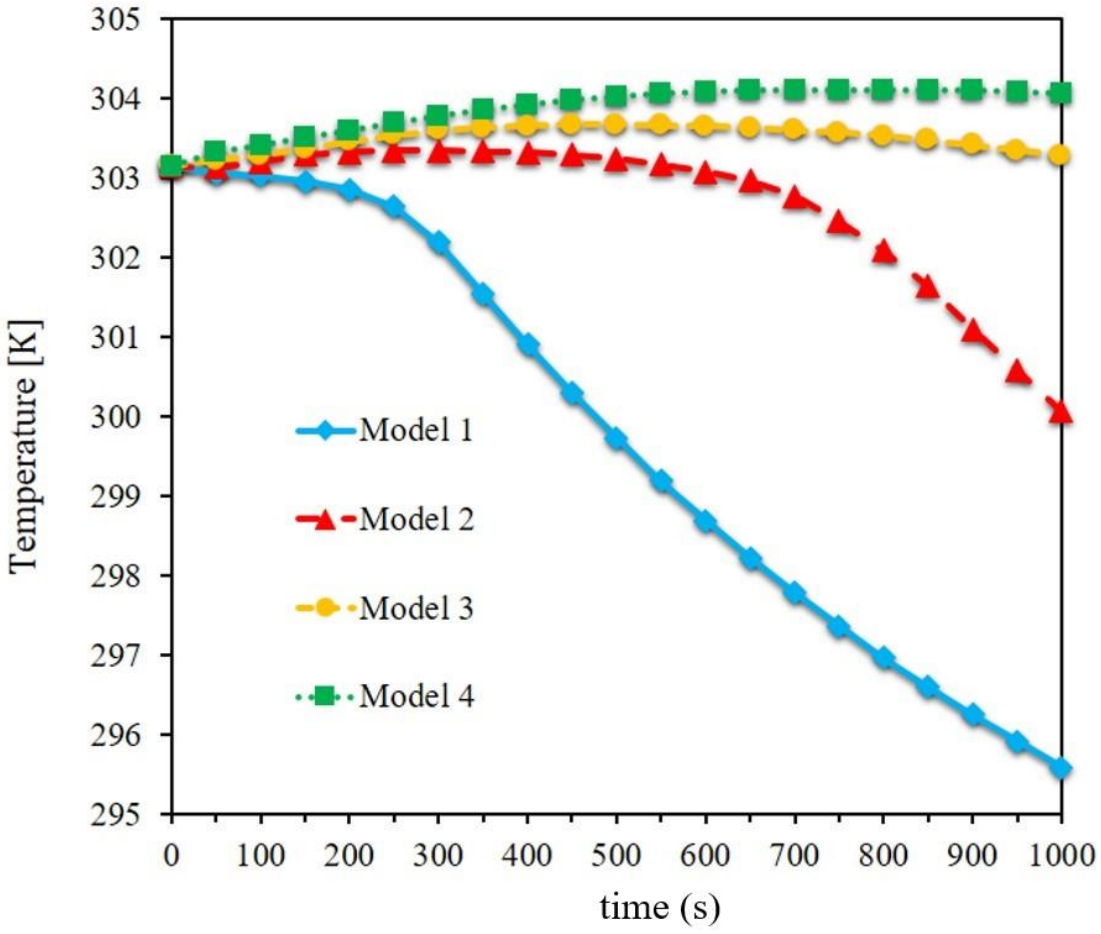


**Figure. 7**. The AVE temperature values of the battery at different times for different aspect ratios of the cavity filled with phase change material.

Figure. 8 shows the AVE temperature of PCM at different times for different PCM heat sink models. The temperature inside the heat sink is lower than in the battery because no energy is generated and only THE is stored as latent heat of fusion. The heat generated in the battery is dissipated to the air via PCM. As long as there is a significant amount of PCM in the liquid phase, the temperature is high because the latent heat of fusion does not cause the temperature of PCM to drop. However, when PCM solidifies, the temperature decreases. Therefore, in heat sink model 1, where the amount of PCM is less and PCM solidifies completely in a shorter time, the temperature of PCM is lower than in other cases. In heat sink model 4, where a higher value of PCM is used and PCM is in the liquid phase for a longer time, the temperature of PCM is slightly higher.

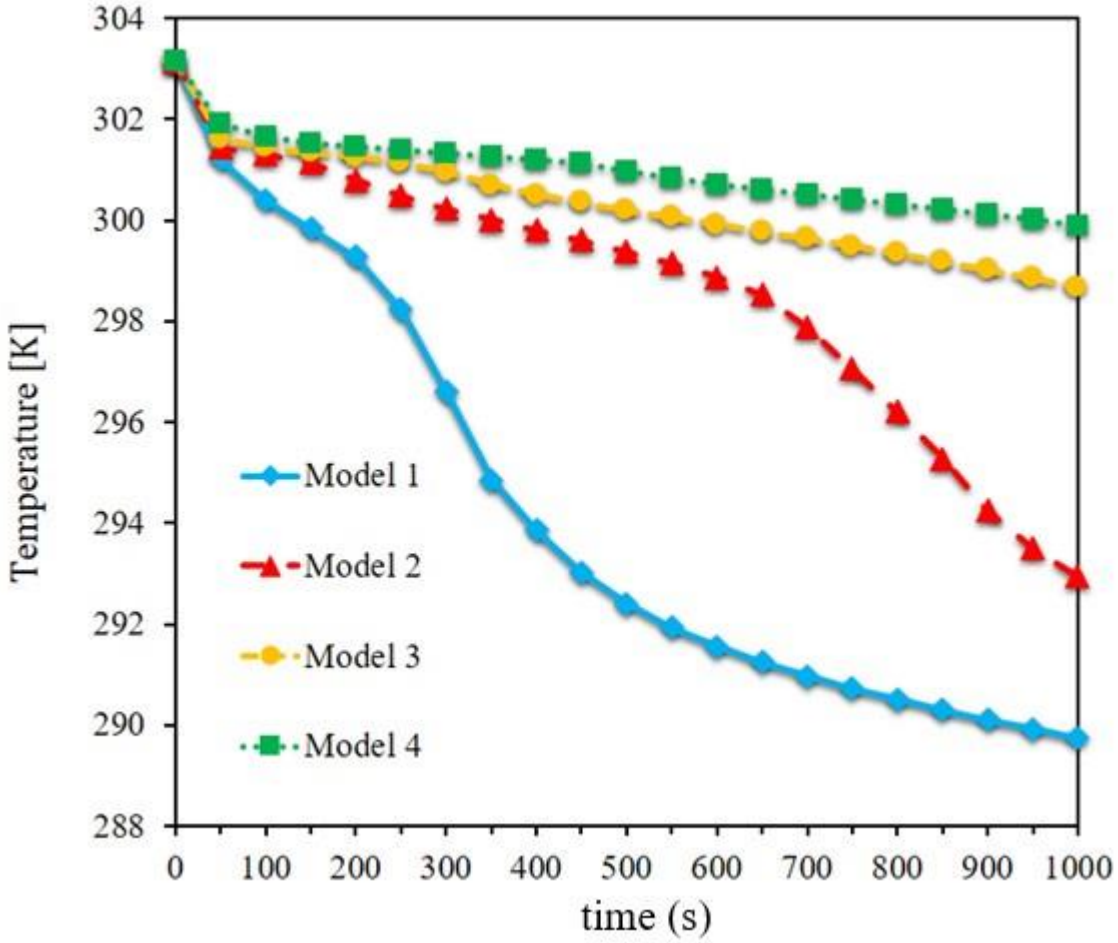


**Figure. 8**. The AVE temperature values of the PCM at different times for different aspect ratios of the cavity filled with phase change material.

Figure 9 shows the MAX T-B at different times for different PCM heat sink models. Due to the shape of the battery in the duct and the collision of the air with one side of the battery, the temperature values in the battery are different, so the temperature at the inlet of the battery is slightly lower than at the outlet. Since the PCM solidifies earlier in the inlet area of the battery, the temperature in this area drops faster, but the temperature in the lower part of the battery is higher for a longer time. MAX Battery temperatures occur in this area. For models with higher PCM thickness, i.e. models 3 and 4, the MAX temperature in the battery cell is slightly higher for a longer period of time. For Model 1, where less PCM is used in the heat sink, the MAX T-B is greatly reduced in a shorter time and the MAX T-B drops sharply.

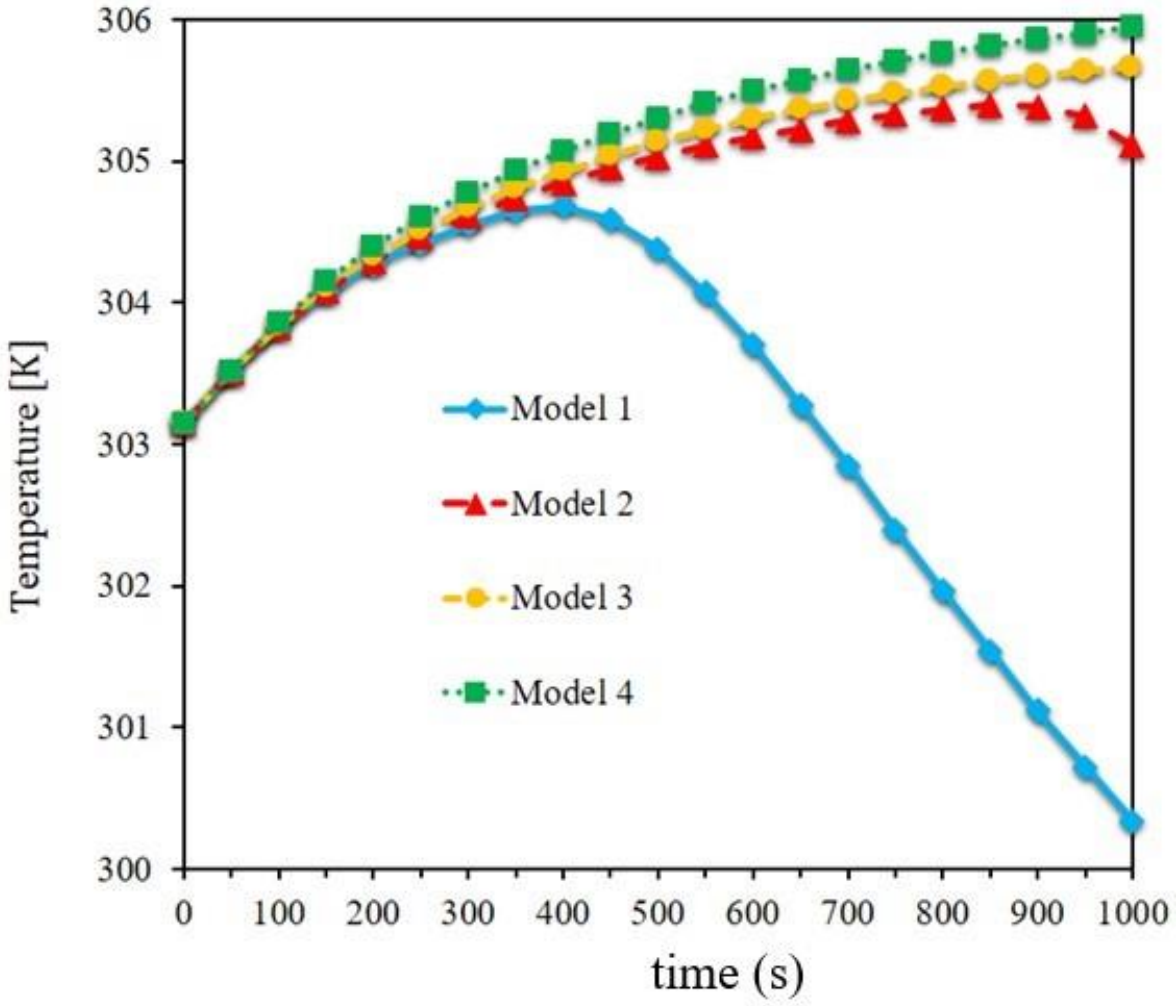


**Figure. 9**. The MAX temperature values of the battery at different times for different aspect ratios of the cavity filled with phase change material.

Figure. 10 shows the values of air outlet temperature at different times for different PCM heat sink models. The air temperature is higher compared to the inlet for two reasons. The first reason is the performance of the battery during the studied period. The battery generates a heat flux due to its chemical reactions. This heat flux causes the air temperature to rise. Also, due to the melting of the entire PCM in the initial period, a large amount of energy is stored in the PCM. As the air passes through the heat sink, some of this energy is transferred to the air. As a result, the air temperature is increased. Also, some of the PCM solidifies by losing its internal energy. Since the dimensions and the type of battery are kept constant for the different heat sink models, the same amount of heat is generated by them. However, due to the different amount of PCM used in the heat sinks of the different models, the amount of energy dissipated to the air is different. Therefore, the MAX amount of air leakage temperature is observed in model 4, which has the highest amount of PCM in the heat sink. In this model, more heat is transferred from PCM

to the air, and consequently the outlet air temperature is higher. Also, the discharge air temperature is higher for a longer time in this model.

The volume fraction of melt PCM is shown in Fig. 11 at different times for different PCM heat sink models. The more PCM used by the battery heat sink, the longer it takes for PCM to completely solidify in the heat sink. Thus, in Model 4, where the PCM heat sink dimensions are larger and more PCM is used around the battery, the PC

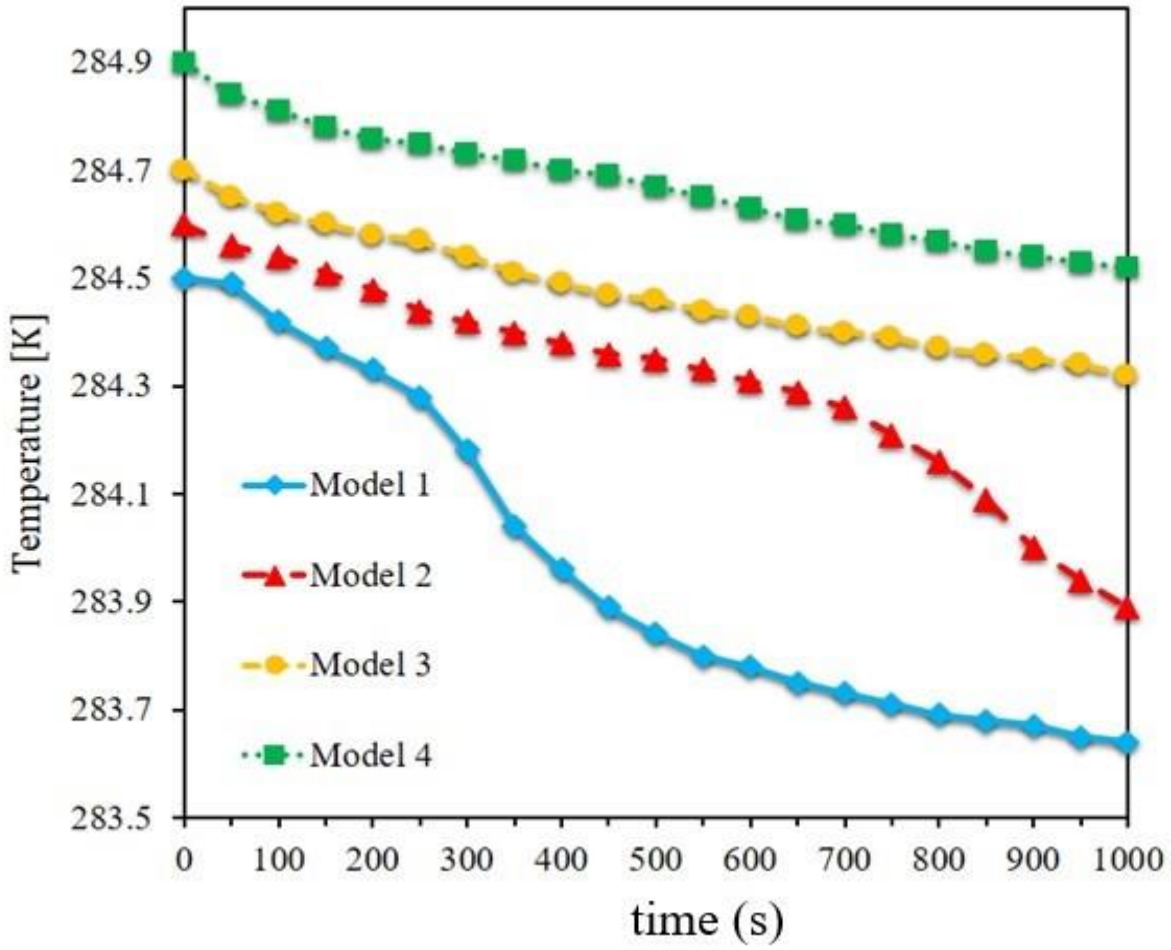


**Figure. 10**. Outlet air temperature values at different times for different aspect ratios of the cavity filled with phase change material.

M solidification time is longer. In contrast, in Model 1, where the heat sink around the battery is smaller and a small amount of PCM is used, PCM solidifies in less than 400 seconds. In Model 2, PCM solidifies in less than 900 seconds, but in Models 3 and 4, some of PCM in the heat sink is still liquid in 1000 seconds. Since the air absorbs the energy stored in the PCM, the amount of solid PCM increases as the air flows with the PCM heat sink for a longer period of time.

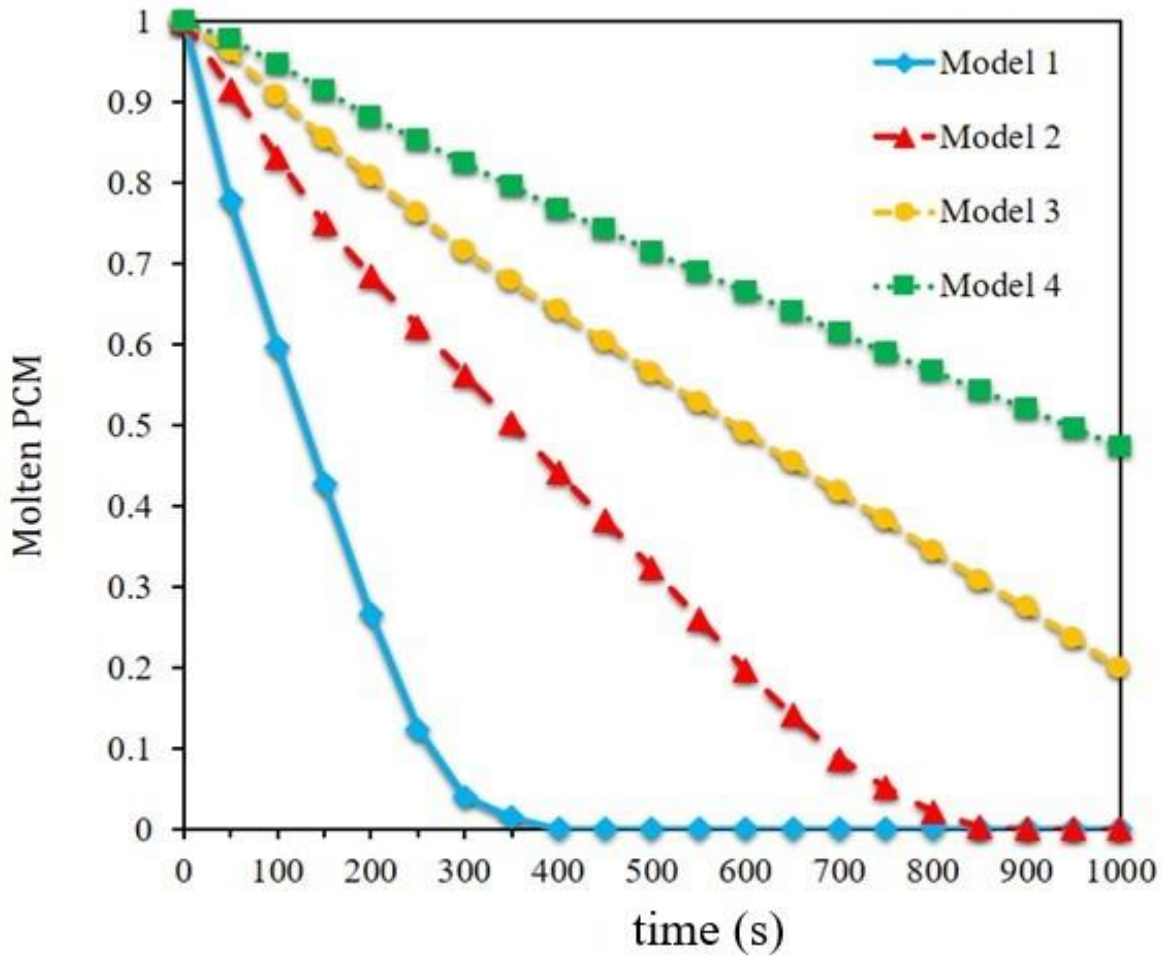


**Figure. 11**. Volume fraction values of molten PCM at different times for different aspect ratios of cavities filled with phase change materials.

In figure. 12, the percentage of energy supplied by the batteries to the annual energy needed to heat the building is shown for two models of the heat sink PCM and a different number of battery cells. Since the amount of THE required in summer is lower and the amount of energy dissipated by the battery cooling system is constant, a significant percentage of the THE required by the building in summer can be supplied by the battery cooling system. In winter, when the building's energy demand is somewhat higher, the amount of energy supplied by the battery cooling system is significantly reduced. Due to the location of the building in a mild climate, the difference between summer and winter temperatures is not very large. In the spring and fall, a moderate amount of the energy required by the building is provided by the battery cooling system. Overall, these improvements and reductions show that 3 to 30% of the building's energy needs can be met by using 5 to 50 battery cells in the battery cooling system. It is also shown that the use of PCM round heat sinks is more suitable for the energy supply of the building than other forms of heat sinks. Due to better heat exchange between air and batteries, the air temperature in this model is higher, which leads to better energy supply than other models. It has more possibilities to increase the amount of energy easily. The air temperature is higher in this model and thus the energy supply is also higher than other models.

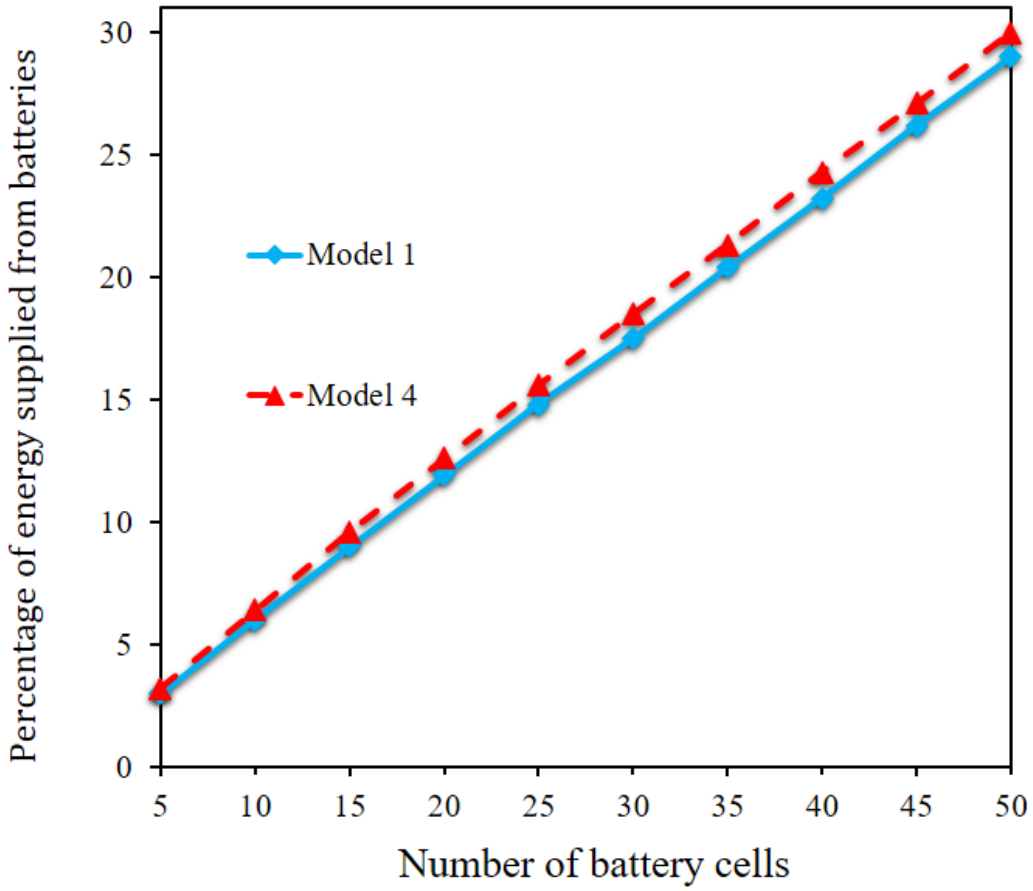


**Figure. 12**. Percentage of energy supplied from heat generated higher than the required heating energy of the building annually for the two aspect ratios of the PCM-filled cavity and the different number of battery cells.

## Conclusions

This paper investigates the effect of using a plate-type lithium-ion battery in the air-conditioning duct of a building to power the building's THE. The batteries are located in a rectangular heat sink with PCM in a laminar air flow. The investigation of different heat sink models leads to the following results.

1- The battery has a lower temperature at the inlet and a higher temperature at the outlet. The MAX -T-B occurs at the outlet.

2- The use of thicker heat sink models leads to an amplification of the MAX -T-B.

3- Model 4 has the MAX average temperature and model 1 has the lowest AVE temperature compared to the other models.

4- Model 4 takes the most time and model 1 takes the least time to completely solidify PCM inside the heat sink.

5- Using 5 to 50 battery cells in the battery cooling system can provide 3 to 30% of the energy needed for the building annually.

## Conflict of Interest

No conflict of interest was declared by the author.

## References

Mert, Mehmet Selçuk, S. E. R. T. Merve, and Hatice Hande MERT. "Isıl enerji depolama sistemleri için organik faz değiştiren maddelerin mevcut durumu üzerine bir inceleme." Mühendislik Bilimleri ve Tasarım Dergisi 6.1 (2018): 161-174.

Gürbüz, Habib, and A. T. E. Ş. Durukan. " Egzoz gazlarını kullanan termal enerji depolama sisteminde RT35 parafin mumunun erime ve katılaşma süreçlerinin sayısal analizi " Mühendislik Bilimleri ve Tasarım Dergisi 9.2 (2021): 520-534.

Al-Zareer, M., Dincer, I., Rosen, M.A., 2017. Novel thermal management system using boiling cooling for high-powered lithium-ion battery packs for hybrid electric vehicles. Journal of Power Sources 363, 291-303.

Almehmadi, F.A., Alqaed, S., Mustafa, J., Jamil, B., Sharifpur, M., Cheraghian, G., 2022. Combining an active method and a passive method in cooling lithium-ion batteries and using the generated heat in heating a residential unit. Journal of Energy Storage 49, 104181.

Alqaed, S., 2022. Effect of annual solar radiation on simple façade, double-skin facade and double-skin facade filled with phase change materials for saving energy. Sustainable Energy Technologies and Assessments 51, 101928.

Amalesh, T., Lakshmi Narasimhan, N., 2020. Cooling of a lithium ion battery using phase change material with air/dielectric fluid media: A numerical study. Proceedings of the Institution of Mechanical Engineers, Part A: Journal of Power and Energy 234(5), 722-738.

An, Z., Jia, L., Ding, Y., Dang, C., Li, X., 2017. A review on lithium-ion power battery thermal management technologies and thermal safety. Journal of Thermal Science 26(5), 391-412.

Bernardi, D., Pawlikowski, E., Newman, J., 1985. A General Energy Balance for Battery Systems. Journal of The Electrochemical Society 132(1), 5-12.

Bibin, C., Vijayaram, M., Suriya, V., Ganesh, R.S., Soundarraj, S., 2020. A review on thermal issues in Li-ion battery and recent advancements in battery thermal management system. Materials Today: Proceedings 33, 116-128.

Elsheikh, M.H., Shnawah, D.A., Sabri, M.F.M., Said, S.B.M., Hassan, M.H., Bashir, M.B.A., Mohamad, M., 2014. A review on thermoelectric renewable energy: Principle parameters that affect their performance. Renewable and sustainable energy reviews 30, 337-355.

Hajatzadeh Pordanjani, A., Aghakhani, S., Afrand, M., Mahmoudi, B., Mahian, O., Wongwises, S., 2019. An updated review on application of nanofluids in heat exchangers for saving energy. Energy Conversion and Management 198, 111886.

Hannan, M.A., Azidin, F., Mohamed, A., 2014. Hybrid electric vehicles and their challenges: A review. Renewable and Sustainable Energy Reviews 29, 135-150.

Huang, Q., Li, X., Zhang, G., Deng, J., Wang, C., 2021. Thermal management of Lithium-ion battery pack through the application of flexible form-stable composite phase change materials. Applied Thermal Engineering 183, 116151.

Huo, Y., Rao, Z., 2015. The numerical investigation of nanofluid based cylinder battery thermal management using lattice Boltzmann method. International Journal of Heat and Mass Transfer 91, 374-384.

Jiang, X., Chen, Y., Meng, X., Cao, W., Liu, C., Huang, Q., Naik, N., Murugadoss, V., Huang, M., Guo, Z., 2022. The impact of electrode with carbon materials on safety performance of lithium-ion batteries: A review. Carbon.

Kalbasi, R., 2021. Introducing a novel heat sink comprising PCM and air - Adapted to electronic device thermal management. International Journal of Heat and Mass Transfer 169, 120914.

Kalbasi, R., Afrand, M., Alsarraf, J., Tran, M.-D., 2019. Studies on optimum fins number in PCM-based heat sinks. Energy 171, 1088-1099.

Kant, K., Shukla, A., Sharma, A., Biwole, P.H., 2017. Heat transfer study of phase change materials with graphene nano particle for thermal energy storage. Solar Energy 146, 453-463.

Karimi, G., Li, X., 2013. Thermal management of lithium-ion batteries for electric vehicles. International Journal of Energy Research 37(1), 13-24.

Khateeb, S.A., Amiruddin, S., Farid, M., Selman, J.R., Al-Hallaj, S., 2005. Thermal management of Li-ion battery with phase change material for electric scooters: experimental validation. Journal of power sources 142(1-2), 345-353.

Khateeb, S.A., Farid, M.M., Selman, J.R., Al-Hallaj, S., 2004. Design and simulation of a lithium-ion battery with a phase change material thermal management system for an electric scooter. Journal of Power Sources 128(2), 292-307.

Kirad, K., Chaudhari, M., 2021. Design of cell spacing in lithium-ion battery module for improvement in cooling performance of the battery thermal management system. Journal of Power Sources 481, 229016.

Lopes, J.A.P., Soares, F.J., Almeida, P.M.R., 2010. Integration of electric vehicles in the electric power system. Proceedings of the IEEE 99(1), 168-183.

Nilsson, M., 2011. Electric vehicles. The Phenomenon of Range Anxiety.

Orooji, Y., Nezafat, Z., Nasrollahzadeh, M., Shafiei, N., Afsari, M., Pakzad, K., Razmjou, A., 2022. Recent advances in nanomaterial development for lithium ion-sieving technologies. Desalination 529, 115624.

Pesaran, A.A., 2001. Battery thermal management in EV and HEVs: issues and solutions. Battery Man 43(5), 34-49.

Pordanjani, A.H., Aghakhani, S., Afrand, M., Sharifpur, M., Meyer, J.P., Xu, H., Ali, H.M., Karimi, N., Cheraghian, G., 2021. Nanofluids: Physical phenomena, applications in thermal systems and the environment effects- a critical review. Journal of Cleaner Production, 128573.

Pordanjani, A.H., Raisi, A., Ghasemi, B., 2019. Numerical simulation of the magnetic field and Joule heating effects on force convection flow through parallel-plate microchannel in the presence of viscous dissipation effect. Numerical Heat Transfer, Part A: Applications 76(6), 499-516.

Qian, Z., Li, Y., Rao, Z., 2016. Thermal performance of lithium-ion battery thermal management system by using mini-channel cooling. Energy Conversion and Management 126, 622-631.

Sanguesa, J.A., Torres-Sanz, V., Garrido, P., Martinez, F.J., Marquez-Barja, J.M., 2021. A review on electric vehicles: Technologies and challenges. Smart Cities 4(1), 372-404.

Shen, Z.-G., Chen, S., Liu, X., Chen, B., 2021. A review on thermal management performance enhancement of phase change materials for vehicle lithium-ion batteries. Renewable and Sustainable Energy Reviews 148, 111301.

Shi, Y., Ahmad, S., Liu, H., Lau, K.T., Zhao, J., 2021. Optimization of air-cooling technology for LiFePO4 battery pack based on deep learning. Journal of Power Sources 497, 229894.

Shojaei, S., Robinson, S., McGordon, A., Marco, J., 2016. Passengers vs. battery: calculation of cooling requirements in a PHEV. SAE Technical Paper.

Singh, L.K., Mishra, G., Sharma, A.K., Gupta, A.K., 2021. A numerical study on thermal management of a lithium-ion battery module via forced-convective air cooling. International Journal of Refrigeration.

Sisk, B., Aliyev, T., Zhang, Z., Jin, Z., Salami, N., Obasih, K., Rick, A., 2015. Integrating thermal and electrochemical modeling of lithium-ion batteries to optimize requirements compliance. SAE Technical Paper.

Sun, X., Li, Z., Wang, X., Li, C., 2019. Technology development of electric vehicles: A review. Energies 13(1), 90.

Tran, M.-K., Panchal, S., Khang, T.D., Panchal, K., Fraser, R., Fowler, M., 2022. Concept Review of a Cloud-Based Smart Battery Management System for Lithium-Ion Batteries: Feasibility, Logistics, and Functionality. Batteries 8(2), 19.

Wang, T., Tseng, K.J., Zhao, J., Wei, Z., 2014. Thermal investigation of lithium-ion battery module with different cell arrangement structures and forced air-cooling strategies. Applied Energy 134, 229-238.

Xie, L., Tang, C., Bi, Z., Song, M., Fan, Y., Yan, C., Li, X., Su, F., Zhang, Q., Chen, C., 2021. Hard Carbon Anodes for Next-Generation Li-Ion Batteries: Review and Perspective. Advanced Energy Materials 11(38), 2101650.

Yang, S., Ling, C., Fan, Y., Yang, Y., Tan, X., Dong, H., 2019. A review of lithium-ion battery thermal management system strategies and the evaluate criteria. International Journal of Electrochemical Science 14(7), 6077-6107.

Yao, M., Gan, Y., Liang, J., Dong, D., Ma, L., Liu, J., Luo, Q., Li, Y., 2021. Performance simulation of a heat pipe and refrigerant-based lithium-ion battery thermal management system coupled with electric vehicle air-conditioning. Applied Thermal Engineering 191, 116878.

Zhang, J., Shao, D., Jiang, L., Zhang, G., Wu, H., Day, R., Jiang, W., 2022. Advanced thermal management system driven by phase change materials for power lithium-ion batteries: A review. Renewable and Sustainable Energy Reviews 159, 112207.

Zhang, X., Li, Z., Luo, L., Fan, Y., Du, Z., 2022. A review on thermal management of lithium-ion batteries for electric vehicles. Energy 238, 121652.

Zhang, Y.S., Courtier, N.E., Zhang, Z., Liu, K., Bailey, J.J., Boyce, A.M., Richardson, G., Shearing, P.R., Kendrick, E., Brett, D.J., 2022. A Review of Lithium-Ion Battery Electrode Drying: Mechanisms and Metrology. Advanced Energy Materials 12(2), 2102233.

Zichen, W., Changqing, D., 2021. A comprehensive review on thermal management systems for power lithium-ion batteries. Renewable and Sustainable Energy Reviews 139, 110685.